

X-932-74-288

PREPRINT

NASA TM X-70776

SIMULATION OF THE GRAVSAT/GEOPAUSE MISSION

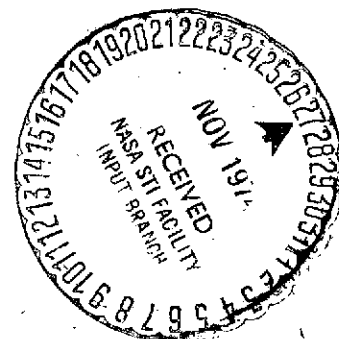
(NASA-TM-X-70776) SIMULATION OF THE
GRAVSAT/GEOPAUSE MISSION (NASA) 26 p HC
\$3.75 CSCI 22B

N75-10980

Unclas
G3/17 02765

DAVID W. KOCH
PETER D. ARGENTIERO

AUGUST 1974



GODDARD SPACE FLIGHT CENTER
GREENBELT, MARYLAND

SUBMITTED FOR PRESENTATION AT THE
AMERICAN GEOPHYSICAL UNION, FALL ANNUAL MEETING,
DECEMBER 12-17, 1974, SAN FRANCISCO, CALIFORNIA

"This paper presents the views of the author(s), and does not necessarily reflect the views of the Goddard Space Flight Center, or NASA."

**For information concerning availability
of this document contact:**

**Technical Information Division, Code 250
Goddard Space Flight Center
Greenbelt, Maryland 20771**

(Telephone 301-982-4488)

SIMULATION OF THE
GRAVSAT/GEOPAUSE
MISSION

David W. Koch
Peter D. Argentiero

August 1974

Submitted for Presentation at the American Geophysical Union,
Fall Annual Meeting, December 12-17, 1974, San Francisco,
California

GODDARD SPACE FLIGHT CENTER
Greenbelt, Maryland

SIMULATION OF THE
GRAVSAT/GEOPAUSE MISSION

David W. Koch
Peter D. Argentiero

ABSTRACT

A simulation of the proposed low Gravsat and high Geopause satellite mission is presented. This mission promises fundamental improvements in the accuracy of low order geopotential coefficients by using satellite-to-satellite tracking technology coupled with a global sampling of the gravity field. Ten days of data from six stations are assumed. A drag compensation system for the low satellite is also postulated. The results show a one to two order of magnitude improvement in the accuracy of the low order coefficients through degree 8 and order 6. Furthermore, these results are easily adjusted to reflect a different data accuracy level and low satellite altitude.

PRECEDING PAGE BLANK NOT FILMED

CONTENTS

	<u>Page</u>
ABSTRACT	iii
INTRODUCTION	1
SIMULATION DESCRIPTION.	3
RESULTS	5
CONCLUSIONS	12
REFERENCES	14
APPENDICES	
1. Covariance Analysis as Applied to Mission Simulation . . .	15
2. NAP/NAPCOV Computer Programs	23

ILLUSTRATIONS

<u>Figure</u>		<u>Page</u>
1	Present Uncertainty of Low Frequency Geopotential	6
2	Improvement Factor in Cosine Term of Geopotential	7
3	Improvement Factor in Sine Term of Geopotential	8
4	Alias Map for Estimate of $C(5,2)$	10
5	Sensitivity of GRAVSAT Velocity to Unit Perturbations of Geopotential Terms (Normed to 300 km) vs GRAVSAT Altitude	11
6	Propagated GRAVSAT Position Errors	13

SIMULATION OF THE GRAVSAT/GEOPAUSE MISSION

INTRODUCTION

NASA's Earth and Ocean Physics Program (EOPAP) is an ongoing effort to apply satellite technology to achieve major advances in the earth and ocean sciences. The prominent feature of the EOPAP is the use of satellites as platforms from which highly accurate instruments globally can sense and monitor a wide range of natural phenomena. The accuracy of these instruments has led to demands for commensurate orbit determination accuracy. As an example, the altimeter scheduled to be on board the GEOS-C spacecraft will have an altitude resolution of 1 to 2 meters. Commensurate altitude determination accuracy of GEOS-C will be difficult to obtain.^{1,2} Another example is the effort to monitor tectonic plate motions by LASER tracking of satellites.³ Again, the major difficulty is the lack of adequate orbit determination accuracy.⁴ It should be mentioned that other missions not directly related to the EOPAP have similar problems. An example is the Earth Observation Satellite (EOS) whose sophisticated imaging equipment cannot be fully exploited until the orbit determination accuracy reaches approximately the 10 meter level.⁵ The major impediment to achieving high orbit determination accuracies is the uncertainty in the low frequency components of the geopotential field. At present these terms are known to about 5% to 50% of their nominal values.⁶ This level of accuracy has been adequate for achieving the sorts of orbit determination accuracies required for previous satellite missions. But a significant improvement in the knowledge of these terms is necessary if the EOPAP is to satisfy its goals. Another and at least equally powerful argument for the pursuit of this improvement is that with a much more accurate geopotential field every satellite mission could be performed less expensively and more efficiently since for a given orbit determination accuracy less tracking data acquisition and processing would be required.

Present Geopotential fields are based on surface gravity measurements and satellite perturbation data. But a set of spherical harmonic coefficients does not achieve orthogonality in non-global blocks of these data types. For geographical and political reasons satellite perturbation data and surface gravity data are not well distributed. Consequently, efforts to estimate spherical harmonic coefficients have been plagued by severe aliasing and a lack of statistical independence. This is essentially an observability problem and no amount of additional data obtained from the same well-covered areas will have a significant effect.

For an accurate satellite determination of the low frequency terms of the geopotential field a dense and globally distributed data set is necessary. This suggests the need for polar satellites in low altitude orbits to insure adequate sensitivity. It is virtually impossible to continuously track such satellites from ground based stations. Thus, satellite-to-satellite tracking using a high relay satellite must be employed. These considerations logically lead to the concept first suggested by Siry⁷ of a dual GRAVSAT/GEOPAUSE mission. The GRAVSAT/GEOPAUSE satellites are to be coplanar in orbits perpendicular to both the earth's equator and the ecliptic plane. The high or GEOPAUSE satellite is placed in a circular orbit at about 3.6 earth radii above the earth's surface. The low or GRAVSAT satellite is placed in a circular orbit about 300 km above the earth's surface. Range rate tracking between GRAVSAT and GEOPAUSE is relayed from GEOPAUSE to ground-based tracking stations. Six properly chosen tracking stations, three in the Northern Hemisphere and three in the Southern Hemisphere, are adequate to maintain constant ground communication with the GEOPAUSE satellite.

The GRAVSAT satellite should be highly sensitive to geopotential variations. But at an altitude of 300 km the effects of atmospheric drag are quite significant and since an adequate model of atmospheric density is unavailable, a drag compensation system is assumed to nullify the effects of atmospheric drag and solar pressure. The spacecraft will consist of two concentric spheres with a combined weight of 2600 lbs. The outer sphere is externally perturbed by both gravitational and nongravitational forces but the inner ball is perturbed by external gravitational forces. In addition, the mutual attraction of the two spheres generates a small internal force. The imbalance in external perturbing forces causes a gradual displacement of the outer sphere relative to the inner sphere. Highly accurate sensors on the interior of the outer sphere detect this displacement and actuate jets to reposition the outer sphere, thus the GRAVSAT is constrained to follow a purely gravitational orbit. The inner sphere is influenced not only by the gravity field of the earth but also by the gravitational attraction exerted by the outer sphere. Imperfect knowledge of this force leads to a certain aliasing of an estimate of geopotential terms and must be accounted for in a realistic error study.

This study reports on a numerical simulation of the GRAVSAT/GEOPAUSE experiment. Ten days of range rate sum data were assumed available. One data point per minute was assumed to be the data acquisition rate and the accuracy was chosen as .2 mm/sec. The fundamental results of the study can be readily scaled to reflect another accuracy level. It was postulated that low frequency coefficients of the spherical harmonic expansion of the geopotential field were estimated from the data. Uncertainties in the orbits of both satellites as well as data biases were included as error sources. The self-gravitation

force of the drag compensated satellite was treated as a constant but unknown force and thus a source of error. The study relies on the techniques of covariance analysis the mathematical basis of which is given in the appendix. What should be mentioned here is that use of these techniques constrains one to the assumption that over the range of uncertainties of the uncertain parameters, the postulated data is a linear function of these parameters.

Attention was focused on the possibilities of extracting from the postulated data estimates of low frequency geopotential terms which are significantly superior to present estimates. Since other experiments such as the installing of a gradiometer or altimeter on board the low satellite could become a part of the GRAVSAT/GEOPAUSE mission, certain orbit determination requirements may be placed on the GRAVSAT satellite. Thus attention was also given to the GRAVSAT orbit determination accuracy which is achievable during this mission.

The results indicate that the GRAVSAT/GEOPAUSE mission is capable of providing the sort of breakthrough in gravity field determination which appears to be required by the EOPAP. And the order of magnitude improvement in gravity field knowledge which this study suggests is possible would significantly reduce the cost of virtually all of NASA's future satellite missions.

SIMULATION DESCRIPTION

The GRAVSAT/GEOPAUSE mission consists of two coplanar satellites in circular orbits of unequal height perpendicular to both the earth's equator and the ecliptic. This coplanarity assures sensing by the GEOPAUSE of both in-plane components of the GRAVSAT orbit. Due to the orbital geometry, the out-of-plane component is weakly observed. When GEOPAUSE is directly above GRAVSAT, the former senses a totally radial component whereas when it trails GRAVSAT by approximately a quarter of a revolution the GEOPAUSE senses a totally along track component. Between these two extremes varying combinations of the two are observed. Such favorable measurement geometry should enable the GEOPAUSE to accurately sense GRAVSAT orbital perturbations. From these perturbations gravity field coefficients can be extracted.

The perpendicularity of the GRAVSAT orbit to the earth's equator guarantees global sampling of the gravity field. The height of the GEOPAUSE is almost two orders of magnitude greater than that of GRAVSAT. This results in near continuous coverage of GRAVSAT by GEOPAUSE. The total sampling of the gravity field by GRAVSAT and its near continuous coverage by GEOPAUSE are two basic strengths of the GRAVSAT/GEOPAUSE mission.

Six ground tracking stations were selected to track GRAVSAT through GEOPAUSE. These stations were selected based upon their ability to provide continuous global tracking of the GEOPAUSE during its tracking of GRAVSAT. Thus a complete well-distributed set of GRAVSAT data is gathered. Such a data set should yield low correlations between estimates of parameters, and subsequent accurate estimates. Three Northern Hemisphere stations (Guam, Madrid, and Rosman) and three Southern (Canberra, Johannesburg, and Santiago) provide such data. Each station observes range sum rate with a one minute integration time over a ten-day span. Measurements are assumed corrupted by a random 0.2 mm/sec noise and a fixed ± 1 mm/sec bias component. These are anticipated state-of-the-art measurement accuracies for the actual mission at the end of the decade.

It is assumed that the total force acting upon the GRAVSAT consists of externally applied atmospheric drag and an internally induced "residual" force. During an actual mission, it is anticipated that this drag will be removed by a surface force compensation system (SFC). Consequently, this report assumes the final result of an application of a SFC system rather than the application of the SFC itself. The "residual" force is due principally to the mutual attraction between the masses of the inner and outer spheres of the GRAVSAT. This force is assumed to be constant and of unknown magnitude but acting solely in the along track direction.

The nominal parameters for the simulation follow:

ORBITS:	GRAVSAT	GEOPAUSE
a(km)	6,678.133	29,431.213
e	0.0	0.0
i(deg)	90.0	90.0
Ω (deg)	90.0	90.0
ω (deg)	180.0	180.0
M(deg)	180.0	180.0
h(km)	300.0	23,053.190
P(hrs)	1.5	14.0

TRACKING STATIONS:

1. Northern Hemisphere: Guam, Madrid, and Rosman
2. Southern Hemisphere: Canberra, Johannesburg, and Santiago

MEASUREMENTS AND UNCERTAINTIES:

Range sum rate at one per minute with 0.2 mm/s noise and ± 1 mm/bias.

PARAMETERS ESTIMATED:

Name	Dimension
GRAVSAT state	6
GEOPAUSE state	6
Measurement bias	6
Residual Force Magnitude	1
Geopotential Coefficients from (0, 0) through (8, 6) inclusive	81

Using the foregoing assumptions, the Navigation Analysis Program, Phase-3, (NAP-3) parameter estimation program^{8,9,10} was used to generate a 100x100 normal matrix of estimated parameters for the ten day data span. Thereafter, the NAP-3 covariance analysis (NAPCOV) program inverted this normal matrix to perform a generalized uncertainty analysis. This analysis consists of varying the treatment of parameters and determining correlations and aliasing properties of the parameters within the normal matrix.

RESULTS

The object of the GRAVSAT/GEOPAUSE mission is to achieve at least an order of magnitude improvement in present knowledge of the low order spherical harmonic coefficients of the geopotential field. In order to determine when a simulation indicates that this goal can be achieved, it is necessary to obtain measures of how well these parameters are known at present. In⁶ the Goddard Earth Model 5 (GEM-5) geopotential field was calibrated against actual observations of 15° by 15° gravity anomalies and nominal standard deviation values were scaled to be consistent with the residuals. The resultant normalized standard deviations as a percent of Kaula's rule of thumb ($10^{-5}/l^2$ where l is the degree of the

spherical harmonic coefficient) are displayed in Figure 1. The results of the GRAVSAT/GEOPAUSE simulation are shown in Figures 2 and 3 as factor improvement numbers. The factor improvement for a given geopotential coefficient is obtained by dividing the present standard deviation of the coefficient as obtained from Figure 1 by the standard deviation obtained from the simulation. Figures 2 and 3 demonstrate that one to two orders of magnitude improvement in present knowledge of the low frequency geopotential field may be expected from the GRAVSAT/GEOPAUSE mission. In addition, the covariance analysis indicated that the estimates of the geopotential coefficients are nearly independent with most correlations between coefficient estimates having absolute values less than 0.01.

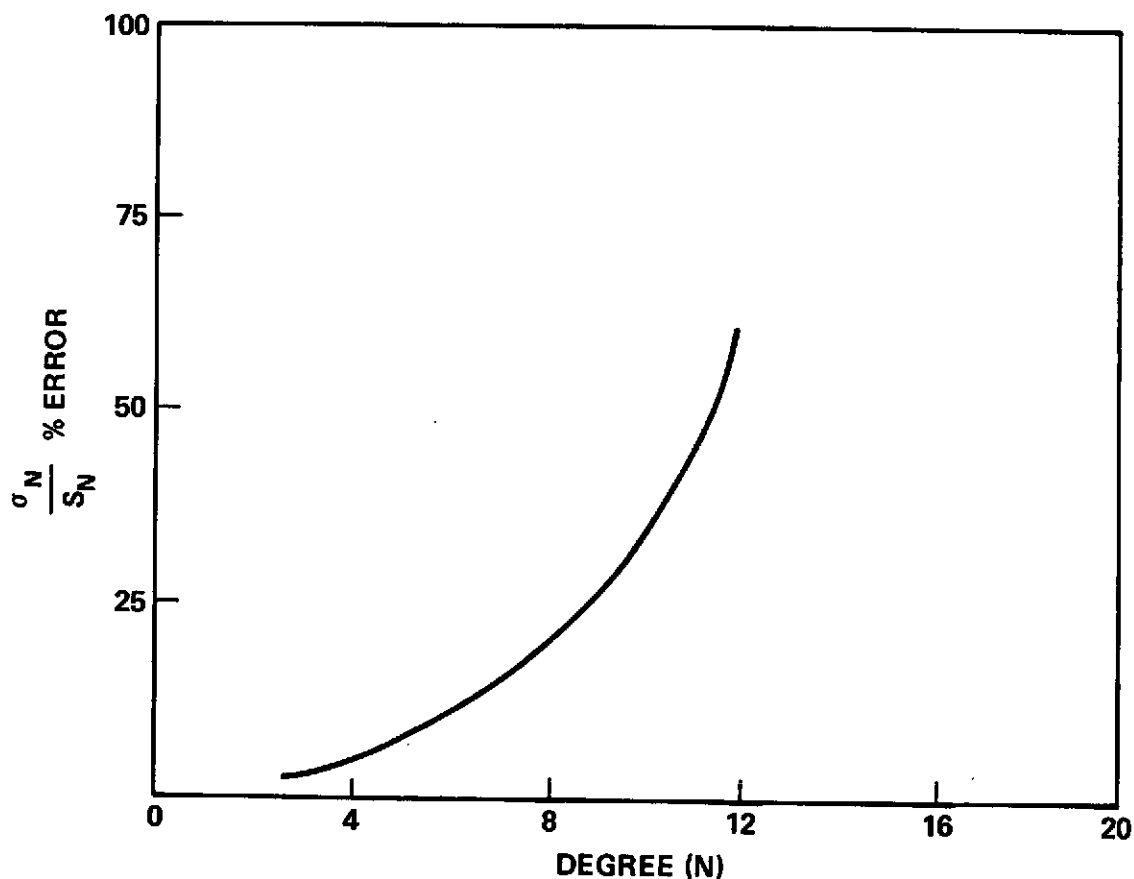


Figure 1. Present Uncertainty of Low Frequency Geopotential

		ORDER (M)						
		0	1	2	3	4	5	6
DEGREE (N)	0	430						
	1	305	915					
	2	424	251	294				
	3	191	152	132	167			
	4	100	68	71	65	93		
	5	131	91	94	92	101	152	
	6	86	59	61	61	64	66	103
	7	129	72	86	73	101	83	352
	8	113	69	78	73	80	80	94

$$\text{IMPROVEMENT FACTOR} = \frac{\text{A PRIORI UNCERTAINTY}}{\text{ESTIMATED UNCERTAINTY}}$$

Figure 2. Improvement Factor in Cosine Term of Geopotential

		ORDER (M)						
		0	1	2	3	4	5	6
DEGREE (N)	0							
	1		915					
	2		255	291				
	3		155	130	166			
	4		70	71	65	94		
	5		92	94	91	100	152	
	6		60	60	60	65	66	
	7		74	85	72	101	83	
	8		70	77	72	80	79	

$$\text{IMPROVEMENT FACTOR} = \frac{\text{A PRIORI UNCERTAINTY}}{\text{ESTIMATED UNCERTAINTY}}$$

Figure 3. Improvement Factor in Sine Term of Geopotential

The results of the simulation as displayed in Figures 2 and 3 are overly optimistic in the sense that the factor improvements do not reflect the aliasing effects of uncertainties in higher frequency geopotential coefficients. In practice, in order to estimate coefficients to degree 8, it would be necessary to estimate the field to a degree higher than 8 and reject the estimates of higher degree coefficients due to aliasing. To gain some knowledge of the aliasing structure of the experiment we simulated an estimation algorithm in which the GRAVSAT and GEOPAUSE states: bias terms, residual force magnitude, and one arbitrarily chosen geopotential term, $C(5,2)$, are estimated. All other geopotential coefficients are left unadjusted at nominal values. The a-priori uncertainty in the unadjusted coefficients were assumed to be those shown in Figure 1. The covariance analysis software (Appendix 1) was employed to determine the root-sum-square contribution to the uncertainty in the unnormalized estimate of $C(5,2)$ due to the uncertainty in each of the unadjusted coefficients. The root-sum-square of the aliasing contributions from the sine and cosine coefficients of a given degree and order were then computed and displayed in the appropriate square of the alias map of Figure 4. The unnormalized a-priori uncertainty of $C(5,2)$ as determined from Figure 1 is approximately 10^{-8} . Figure 4 shows that uncertainties in terms of degree as high as 8 have non-negligible contributions to uncertainties in estimates of terms of degree 5. This indicates that good estimates of geopotential coefficients are obtained when estimated terms are separated from unestimated terms by at least 4 degrees. Hence, for a good determination of the field to degree and order 8, a field of degree and order 12 should be estimated from the data and estimates of terms of degree 9 through 12 discarded due to aliasing.

For this simulation the GRAVSAT satellite was assumed to be in a circular orbit with altitude 300 km. Since a higher altitude would have a favorable impact on orbital lifetime and fuel requirements it is useful to scale the results of Figures 2 and 3 to reflect the experiment results when a higher altitude is chosen for GRAVSAT. Figure 5 shows the sensitivity of GRAVSAT velocity to unit perturbations of geopotential terms (normed to 300 km) versus GRAVSAT altitude. Provided that statistical independence of estimates is maintained, the ratio of standard deviations of estimates of the same geopotential coefficient at two different GRAVSAT heights should be inversely proportional to the ratio of their sensitivities in GRAVSAT velocity data at the two heights. Consider any geopotential term of degree 8. Its standard deviation at 500 km will be equal to its standard deviation at 300 km scaled by the ratio of GRAVSAT velocity sensitivity of 300 km to 500 km. Figure 5 shows that for such terms, the standard deviations of their estimates increase by a third if the GRAVSAT altitude is raised from 300 km to 500 km. This suggests that the mission is feasible at a 500 km GRAVSAT altitude although the statistical independence of the estimates would be somewhat compromised at the higher altitude. It also

should be mentioned that the results displayed in Figures 2 and 3 are inversely proportional to the assumed standard deviation (.2 mm/sec) of the range rate sum data. Thus, the results can be readily scaled to reflect another accuracy level.

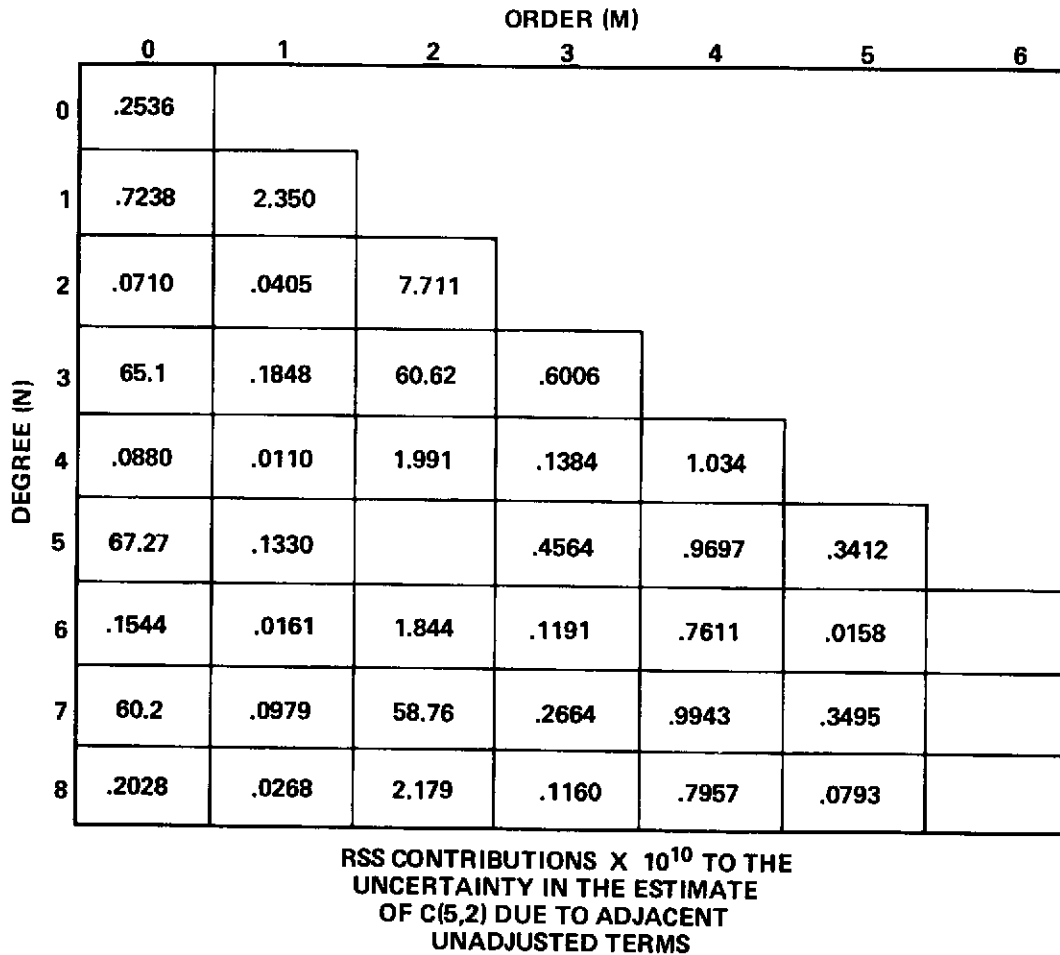


Figure 4. Alias Map for Estimate of C(5,2)

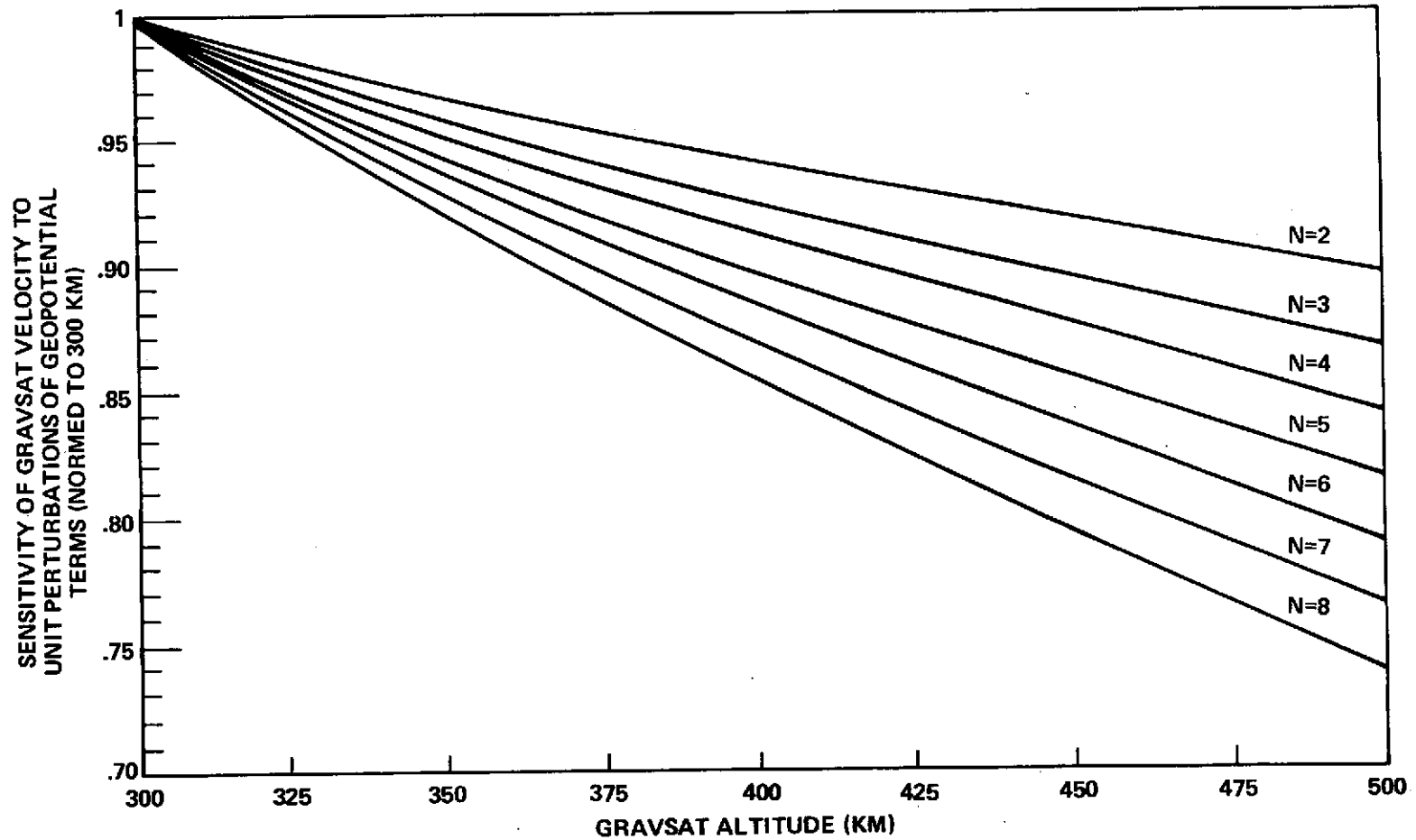


Figure 5. Sensitivity of GRAVSAT Velocity to Unit Perturbations of Geopotential Terms (Normed to 300 km) vs GRAVSAT Altitude

Since the GRAVSAT satellite is configured to be in a low polar orbit, the mission should be attractive to other experimenters. The inclusion of an altimeter or gradiometer are definite possibilities. Consequently, our ability to recover GRAVSAT state at various times is important. Figure 6 provides the radial, along track, and cross track position errors of GRAVSAT as a function of time from epoch. These errors include the effect of errors in a-posteriori estimates of geopotential coefficients to degree 8 but do not reflect the effect of uncertainties in estimates of geopotential coefficients of degree greater than 8. If the effects of uncertainties in higher degree terms were included in the error propagations of Figure 6, the uncertainties in GRAVSAT position could increase by as much as an order of magnitude. Notice also that the cross track component of GRAVSAT since it is weakly observed by the coplanar GEOPAUSE satellite, cannot be estimated as accurately as the along track and radial components.

CONCLUSIONS

The GRAVSAT/GEOPAUSE mission configuration is capable of producing a global distribution of observations of along track and radial perturbations of the GRAVSAT satellite. Six tracking stations, three in the Northern Hemisphere, and three in the Southern Hemisphere are adequate to maintain constant communication with the GEOPAUSE satellite. This insures a global distribution of data. Assuming 10 days of range rate sum data with a .2 mm/sec accuracy for a 1 minute integration time, the results of this report show that an order of magnitude improvement in knowledge of low frequency geopotential coefficients can be realized. The resultant estimates should be nearly independent with most correlations of absolute value less than .01. The aliasing effects of higher order terms are still considerable, however, and if a spherical harmonic field of degree and order N is to be estimated, a field complete to at least degree and order $N + 4$ must be adjusted in a standard least squares sense.

These results assume a GRAVSAT altitude of 300 km. A sensitivity analysis indicates that uncertainties in estimates of geopotential coefficients to degree 8 would increase by about a third if the GRAVSAT altitude were increased to 500 km. Some degradation in the statistical independence of coefficient estimates would also be experienced at the higher altitude.

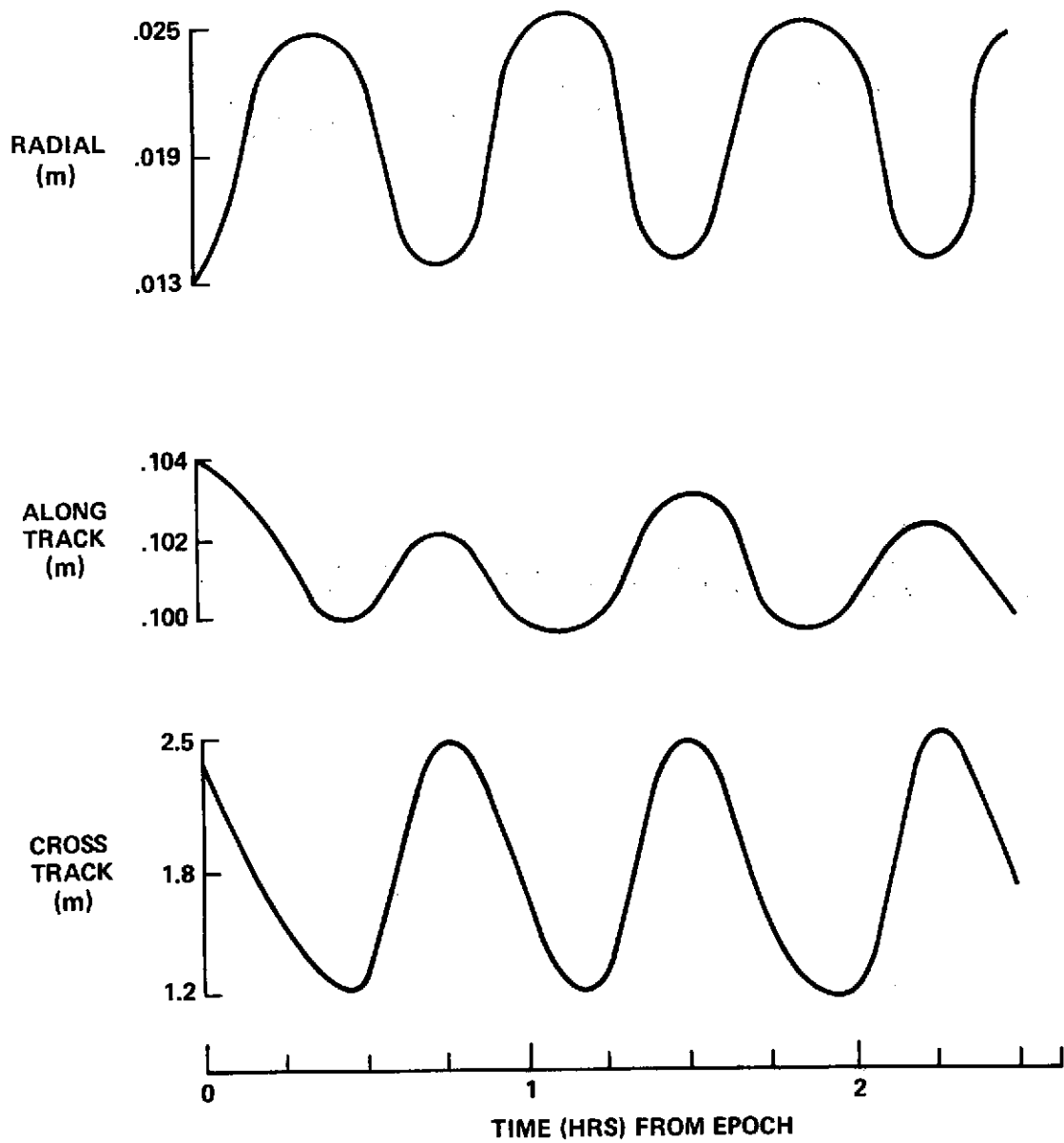


Figure 6. Propagated GRAVSAT Position Errors

REFERENCES

1. D. Koch, P. Argentiero and W. D. Kahn. "Long and Short Arc Altitude Determination for GEOS-C." NASA/GSFC X-591-73-368. November 1973.
2. P. Argentiero and R. Garza-Robles. "GEOS-C Orbit Determination With Satellite-to-Satellite Tracking." NASA/GSFC X-932-74-133. May 1974.
3. "Earth and Ocean Physics Applications Program." Rationale and Program Plans. Volume II. NASA. September 1972.
4. Russell W. Agreen and David E. Smith. "A Simulation of the San Andreas Fault Experiment." NASA/GSFC X-592-73-216. May 1973.
5. "Earth Observatory Satellite (EOS)." Definition Phase Report. Volume I. Goddard Space Flight Center, Greenbelt, Maryland, August 1971.
6. F. J. Lerch, C. A. Wagner, J. E. Brownd and J. A. Richardson. "Goddard Earth Models 5 and 6." NASA/GSFC X-921-74-145. September 1974.
7. Joseph W. Stry. "A GEOPAUSE Satellite System Concept." NASA/GSFC X-550-71-503. April 1971.
8. J. J. Lynn, J. G. Hartwell and R. S. Nankervis. "Network Analysis Program, NAP-3, Mathematical Analysis Documentation." DBA Systems, Inc. June 1, 1970.
9. R. Garza-Robles, S. Guion, T. Lewis and D. Lynn. "Network Analysis Program, NAP-3, Program Analysis Documentation." DBA Systems, Inc. June 1, 1970.
10. "User's Guide to Data Preparation Navigation Analysis Program, (NAP 3.1)." Old Dominion Systems, Inc. April 1974.
11. J. J. Lynn. "NAPCOV Program Documentation." Old Dominion Systems, Inc. November 1973 (revised May 1, 1974).

APPENDIX 1

COVARIANCE ANALYSIS AS APPLIED TO MISSION SIMULATION

COMPUTING COVARIANCE MATRICES

Let $\tilde{y}(m)$ be an m dimensional vector consisting of the differences between the correct values of observations of a satellite and nominal values of the observations as determined from a nominal orbit. Also let $\tilde{z}(n)$ be an n dimensional vector of differences between actual and nominal values of the state of the satellite at an epoch and differences between actual and nominal values of parameters in the dynamic and measurement models whose associated uncertainties may limit our ability to estimate satellite state from the data. The sensitivity matrix $c(m, n)$ is defined as that matrix whose element in the i th row and the j th column is the partial derivative of $\tilde{y}(i)$ with respect to $\tilde{z}(j)$. A first order Taylor series expansion of the functional relationship between \tilde{y} and \tilde{z} about the nominal value of \tilde{z} yields

$$\tilde{y} = c\tilde{z} \quad (\text{A-1})$$

An orbit determination program in processing observations y of \tilde{y} to obtain a least square adjustment to \tilde{z} computes a so-called normal matrix defined as

$$\eta(n, n) \equiv c^T w c \quad (\text{A-2})$$

where w is a weighting matrix and is usually the inverse of the covariance matrix of the observations y of \tilde{y} . Once an orbit determination program computes and stores the normal matrix, a number of questions can be raised and answered at very little cost in terms of computation time.

The best estimate of the state of the satellite at epoch is obtained by performing a least squares adjustment of the state at epoch and all other parameters with which are associated significant uncertainties. But frequently this straightforward approach leads to severe core storage requirements. In practice some of the parameters in the dynamic and measurement models are estimated along with state and others are fixed at their nominal values and left unadjusted in the least squares process. In order to determine the consequences of estimating some parameters and ignoring others it is useful to compute the covariance matrix of such a least squares estimation procedure.

Let \tilde{z} be decomposed into two disjoint parameter sets as follows

$$\tilde{z} = \begin{bmatrix} \tilde{x}_1(n_1) \\ \tilde{x}_2(n_2) \end{bmatrix} \quad (\text{A-3})$$

where \tilde{x}_1 , is a set of n_1 , parameters which are to be estimated in a least squares process and \tilde{x}_2 is a set of n_2 parameters whose nominal values are left unadjusted by the least squares process but whose uncertainties are to be considered in computing the covariance matrix of the resulting estimator. Define a matrix $A(m, n_1)$ as a matrix whose element in the i th row and j th column is the partial derivative of $\hat{y}(i)$ with respect to $x_1(j)$. Analogously define $B(m, n_2)$ as the matrix whose element in the i th row and j th column is the partial derivative of $\tilde{y}(i)$ with respect to $x_2(j)$. For future reference notice that the normal matrix η of \tilde{z} as computed and stored by an orbit determination program and defined by Equation A-2 can be written as

$$\eta = \begin{bmatrix} A^T w A & A^T w B \\ B^T w A & B^T w B \end{bmatrix} \quad (\text{A-4})$$

Assume that there exists a priori estimates of \tilde{x}_1 and \tilde{x}_2 with properties

$$\begin{aligned} x_1' &= \tilde{x}_1 + \alpha_1, & E(\alpha_1) &= \bar{0}, & E(\alpha_1 \alpha_1^T) &= P_1 \\ x_2' &= \tilde{x}_2 + \alpha_2, & E(\alpha_2) &= \bar{0}, & E(\alpha_2 \alpha_2^T) &= P_2 \end{aligned}$$

and assume that the observation vector y or \tilde{y} has properties

$$y = \tilde{y} + \nu, \quad E(\nu) = \bar{0}, \quad E(\nu \nu^T) = w^{-1}$$

The least squares estimate of \tilde{x}_1 is obtained as the value of \tilde{x}_1 which minimizes the loss function

$$L(x_1) = (y - Ax_1 - Bx_2')^T w (y - Ax_1 - Bx_2') + (x_1' - x_1)^T P_1^{-1} (x_1' - x_1) \quad (\text{A-5})$$

The resulting least squares estimator of \tilde{x}_1 is well known to be

$$\hat{x}_1 = (A^T w A + P_1^{-1})^{-1} [A^T w (y - B x_2') + P_1^{-1} x_1'] \quad (A-6)$$

Define

$$P = [E (\hat{x}_1 - \tilde{x}_1) (\hat{x}_1 - \tilde{x}_1)^T] \quad (A-7)$$

A series of substitutions reveals that

$$\hat{x}_1 - \tilde{x}_1 = (A^T w A + P_1^{-1})^{-1} (-A^T w B \alpha_2 + A^T w \nu + P_1^{-1} \alpha_1) \quad (A-8)$$

Equation 8 yields

$$P = (A^T w A + P_1^{-1})^{-1} + (A^T w A + P_1^{-1})^{-1} A^T w B P_2 B^T w A (A^T w A + P_1^{-1})^{-1} \quad (A-9)$$

Notice that the right side of Equation 9 can be computed if one has a priori covariance matrices P_1 and P_2 , and the upper right and upper left portions of the normal matrix. To determine the covariance matrix of an estimator which estimates some subset of \tilde{z} other than \tilde{x}_1 , all that is necessary is to permute the rows and columns of η in the appropriate fashion and proceed as before. Thus if one assumes that the normal matrix defined by Equation 2 is precomputed it becomes an easy matter to obtain the resultant covariance matrix when any subset of the \tilde{z} parameters are estimated in a least squares sense and the rest are ignored.

THE ALIAS MATRIX

Assume that all the data has the same variance. Hence

$$w = (I \sigma_0^2)^{-1} \quad (A-10)$$

where σ_0^2 is the common variance of each data point. Also assume that the a priori estimates of the unadjusted parameters are independent. Under this

assumption the covariance matrix P_2 of x_2' can be written as

$$P_2 = \begin{bmatrix} \sigma_1^2 & & & 0 \\ & \sigma_2^2 & & \\ & & \ddots & \\ 0 & & & \sigma_n^2 \end{bmatrix} \quad (A-11)$$

where σ_i^2 is the a priori variance of the i th unadjusted parameter. Also define a matrix $K(n_1, n_2)$ as

$$K = (A^T w A)^{-1} A^T w B \quad (A-12)$$

With these assumptions Equation 9 yields the following expression for the i th diagonal element of P

$$P(I, I) = \sum_{j=0}^{n_2} (\beta_{i,j} \sigma_j)^2 \quad (A-13)$$

where $\beta_{i,0}$ is the i th diagonal element of the matrix $(A^T A)^{-1}$ (this assumes that diagonal elements of the matrix P_1^{-1} are relatively small) and

$$\beta_{i,j} = K(i, j), \quad j \geq 1 \quad (A-14)$$

The standard deviation of the i th estimated parameter is given by

$$\sigma_i = \left(\sum_{j=0}^{n_2} (\beta_{i,j} \sigma_j)^2 \right)^{1/2} \quad (A-15)$$

Define the error sensitivity matrix as

$$S = \{ \beta_{i,j} \}, \quad i = 1, 2, \dots, n_1, \quad j = 0, 1, \dots, n_2 \quad (A-16)$$

And finally define the Alias Matrix as

$$L = \bar{S}\bar{\sigma} \quad (\text{A-17})$$

where

$$\bar{\sigma} = \begin{bmatrix} \sigma_0 & & & 0 \\ & \sigma_1 & & \\ & & \ddots & \\ 0 & & & \sigma_{n_2} \end{bmatrix} \quad (\text{A-18})$$

The standard deviation of the i th estimated parameter is seen to be the root sum square of the terms in the i th row of the alias matrix. The elements in the first column of the alias matrix represent the RSS contribution to the standard deviation of each estimated parameter due to the data noise. The elements in the j th column, $j \geq 2$, represent the RSS contribution to the standard deviation of each estimated parameter due to the $j - 1$ st unadjusted parameter.

Possession of the alias matrix reveals much of the probability structure of the postulated least squares estimator. With this information one can quickly determine which error sources are significant with regard to the estimation of a given parameter.

Propagating Covariance Matrices

Equation 9 provides the covariance matrix of the state $\tilde{\mathbf{x}}_1$ at some specified epoch. In many cases it is important to determine how accurately the state can be determined at some time other than epoch. In order to do this correctly it is necessary to take into proper account uncertainties in dynamic parameters. These parameters may be in an estimated mode or in an unadjusted mode and to incorporate their effect one resorts to state transition matrices which presumably have been precomputed by an orbit determination program. Let $\tilde{\mathbf{x}}_1(T)$ be the estimated state at time T . Assume as output from an orbit determination program the state transition matrices

$$\bar{v}_1(T) = \frac{\partial \tilde{\mathbf{x}}_1(T)}{\partial \tilde{\mathbf{x}}_1}, \quad \bar{v}_2(T) = \frac{\partial \tilde{\mathbf{x}}_1(T)}{\partial \tilde{\mathbf{x}}_2} \quad (\text{A-19})$$

If there are no dynamic parameters in the estimation vector $\tilde{\mathbf{x}}_1$, the matrix $\bar{\mathbf{v}}_1 (T)$ takes on the particularly simple form,

$$\bar{\mathbf{v}}_1 (T) = \begin{bmatrix} \delta & 0 \\ 0 & \mathbf{I} \end{bmatrix} \quad (\text{A-20})$$

where δ is the six by six matrix defined as the partial derivative matrix of the state of the satellite at time T with respect to the state of the satellite at epoch. If dynamic parameters are included in the estimated state, the off diagonal matrices become non-zero and $\bar{\mathbf{v}}_1 (T)$ assumes a more complicated form. The matrix $\bar{\mathbf{v}}_2 (T)$ is the matrix of partial derivatives of the state $\tilde{\mathbf{x}}_1 (T)$ with respect to the unadjusted parameters $\tilde{\mathbf{x}}_2$. If no dynamic parameters are in the unadjusted mode, $\bar{\mathbf{v}}_2 (T)$ is the null matrix. A first order Taylor series expansion of the function which describes the time evolution of the state $\tilde{\mathbf{x}}_1 (T)$ yields

$$\tilde{\mathbf{x}}_1 (T) = \bar{\mathbf{v}}_1 (T) \tilde{\mathbf{x}}_1 + \bar{\mathbf{v}}_2 (T) \tilde{\mathbf{x}}_2 \quad (\text{A-21})$$

Substituting $\hat{\mathbf{x}}_1$ as obtained from Equation 6 for $\tilde{\mathbf{x}}_1$ and \mathbf{x}_2' for $\tilde{\mathbf{x}}_2$ provides the best estimate $\hat{\mathbf{x}}_1 (T)$, of $\tilde{\mathbf{x}}_1 (T)$

$$\hat{\mathbf{x}}_1 (T) = \bar{\mathbf{v}}_1 (T) \hat{\mathbf{x}}_1 + \bar{\mathbf{v}}_2 (T) \mathbf{x}_2' \quad (\text{A-22})$$

The covariance matrix of $\hat{\mathbf{x}}_1 (T)$ is given by

$$\begin{aligned} \mathbf{P} (T) = & \bar{\mathbf{v}}_1 (T) \mathbf{P} \bar{\mathbf{v}}_1^T (T) + \bar{\mathbf{v}}_2 (T) \mathbf{P}_2 \bar{\mathbf{v}}_2^T (T) + \bar{\mathbf{v}}_1 (T) \mathbf{E} [\hat{\mathbf{x}}_1 \mathbf{x}_2'] \bar{\mathbf{v}}_2 (T) \\ & + \bar{\mathbf{v}}_2 (T) \mathbf{E} [\mathbf{x}_2' \hat{\mathbf{x}}_1^T] \bar{\mathbf{v}}_1^T (T) \end{aligned} \quad (\text{A-23})$$

Equation 23 in conjunction with Equations 6 and 9 yields

$$\begin{aligned} \mathbf{P} (T) = & \bar{\mathbf{v}}_1 (T) (\mathbf{A}^T \mathbf{w} \mathbf{A} + \mathbf{P}_1^{-1})^{-1} \bar{\mathbf{v}}_1^T (T) + \left[\bar{\mathbf{v}}_1 (T) (\mathbf{A}^T \mathbf{w} \mathbf{A} + \mathbf{P}_1^{-1})^{-1} \mathbf{A}^T \mathbf{w} \mathbf{B} \right. \\ & \left. - \bar{\mathbf{v}}_2 (T) \right] \mathbf{P}_2 \left[\bar{\mathbf{v}}_1 (T) (\mathbf{A}^T \mathbf{w} \mathbf{A} + \mathbf{P}_1^{-1})^{-1} \mathbf{A}^T \mathbf{w} \mathbf{B} - \bar{\mathbf{v}}_2 (T) \right]^T \end{aligned} \quad (\text{A-24})$$

Finally notice that in much the same fashion that Equation 9 was used to develop an alias matrix at epoch, Equation 24 can be utilized to develop an alias matrix for any time T.

REMARKS

If one possesses a functioning orbit determination program it becomes a relatively easy matter to add covariance analysis capability to the system. A computer program can be written which assumes as input a normal matrix and state transition matrices as generated by the orbit determination program. By permuting the rows and columns of the normal matrix and completing the matrix operations defined by Equation 9, the covariance matrix of a least square process which adjusts any subset of the parameters and ignores the rest can be computed. An alias matrix can be obtained and significant error sources can be identified. By utilizing the precomputed state transition matrices, the covariance matrix of the estimate of the state can be propagated from epoch to any other time. These operations are very simple and they consume little computer time.

Since the normal matrix and state transition matrices are computed once and permanently stored, it is possible to investigate a large number of possible estimation strategies. This can be done conveniently and cheaply. For many applications such a program is a useful and quickly developed addition to an orbit determination system.

APPENDIX 2

NAP/NAPCOV COMPUTER PROGRAMS

The Navigation Analysis Program, Phase-3, (NAP-3),^{8,9,10} is a conventional parameter estimation program which utilizes a least squares iterative process to extract estimates and uncertainties of parameters from data and initial estimates of these parameters. The program can process data of 26 different types of measurements to estimate as many as 30 different types of parameters. A maximum of 100 individual parameters can be estimated. NAP-3 can also simulate the orbit determination process in which only uncertainties of selected are estimated. This particular program is the latest version of a series of estimation programs starting with the GEOS Data Adjustment Program (GDAP), NAP-1, and NAP-2.

NAP-3 is divided into three functional modules: Data Edit, Partials, and Solver. Information between the three is passed via common blocks and/or files. Data Edit checks and organizes the input data and outputs initial conditions. The Partials module integrates the nominal trajectory, computes measurements, generates partial derivatives of each measurement with respect to each parameter to be estimated, and computes measurement discrepancies. The third and final module, Solver, receives these partial derivatives and discrepancies to form and solve the normal equations. Convergence tests occur at this point. Upon convergence the final estimate and its uncertainties are output. Thereupon a square normal matrix is passed to the NAP-3 Covariance Analysis (NAPCOV) Program.¹¹ The NAPCOV program inverts this matrix and by manipulating appropriate rows and columns can partition the parameters within the normal matrix into "solve for" and "consider" categories. Thus the user has the flexibility to rearrange the parameters to his choosing and determine the effects of the "consider" upon the "solve for" parameters. Furthermore the program computes correlations and the "aliasing" or degrading effect upon certain parameters. Together the NAP and NAPCOV programs allow the user to perform in-depth analysis of a wide variety of parameter estimation problems.

PRECEDING PAGE BLANK NOT FILMED